PREDICTION OF RESIDUAL STRENGTH OF PANELS AND SHELLS

W. Brocks[a], I. Scheider[b]

[a] *Materials Mechanics, Institute of Materials Research, GKSS Research Centre, D – 21502 Geesthacht (Germany), e-mail:wolfgang.brocks@gkss.de*
[b] *e-mail:ingo.scheider@gkss.de*

ABSTRACT
A cohesive model for ductile crack extension is used for numerical analyses of the mechanical behaviour of metal sheets with cracks and particularly for assessments of the residual strength of panels and shells under quasi-static loading. After describing how the characteristic parameters are determined, the model is applied to various specimen configurations and structural components. The excellent numerical performance favours the application for predicting the residual strength of lightweight components like aircraft fuselages.

1. INTRODUCTION

Present-day aircraft design is based on a damage tolerance concept, which acknowledges the existence of cracks and structural damage. The construction has to be designed in a way that any crack extension during service will not lead to catastrophic failure within the inspection intervals. The prediction of the residual strength of stiffened and un-stiffened thin-walled panels and shells in aircraft structures is an essential part of any damage tolerance analysis. Typical characteristics, which a respective failure assessment concept has to take into account, are

- Pronounced stable crack extension prior to failure and
- Constraint effects and related issues, which make any application of standard test methods for fracture toughness impossible or too conservative.

As the plane-strain assumption of classical fracture mechanics restricts its application to heavy-section structures, analytical and numerical methods for predicting crack extension have been specifically adapted to thin-walled structures, for instance R-curve approaches based on the crack tip opening displacement (CTOD) or the crack-tip opening angle (CTOA) [1 - 3].
In the present contribution, the application of cohesive models for numerical analyses of ductile crack extension in metal sheets in order to predict the mechanical behaviour and particularly the residual strength of shell structures under quasi-static loading is addressed. Cohesive models are used for numerical crack propagation analyses on various length scales for several decades now. They are used as interfaces in finite element analyses, which represent the damage and failure properties of the material. As the crack can extend along the boundaries of solid elements, only, the crack path is predefined by the mesh Thus, interface elements are only advantageous, if there is a limited number of alternatives for the crack to extend, i.e. in bifurcation problems. Such problems play an important role in the frame of structural integrity analyses, however.

2. THE COHESIVE MODEL

2.1 Model Description

Dugdale [4] and Barenblatt [5] introduced a cohesive zone ahead of the crack tip in order to avoid the unrealistic infinite stress at the crack tip, which is characteristic of the stress intensity factor approach. Modern phenomenological cohesive models (CM) describe various kinds of decohesion processes; Fig. 1, by a relation between a vector of surface tractions or cohesive stresses $\sigma^T = \{\sigma_n, \sigma_t, \sigma_s\}$,

having one normal and two tangential components and a vector of the material separation, $\delta^{\mathrm{T}} = [\mathbf{u}]^{\mathrm{T}} = \{\delta_{\mathrm{n}}, \delta_{\mathrm{t}}, \delta_{\mathrm{s}}\}$. Cohesive surface elements are introduced at the boundaries of solid elements along a pre-defined crack path. Various functions for the cohesive law or traction-separation law (TSL), $\sigma = \mathbf{f}(\delta)$, and numerous applications exist in the literature, see the overview given in [6]. Cohesive elements have in particular proven their ability in modelling crack extension in thin-walled panels [7 - 9].

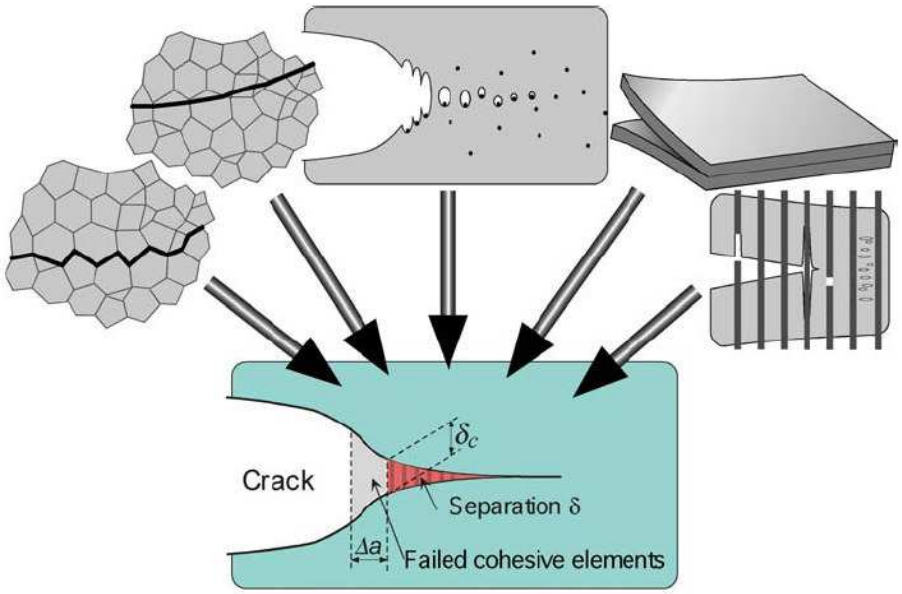

Fig. 1 - Schematic of a cohesive zone in a continuum representing various separation mechanisms

The phenomenological TSL represents the effective mechanical behavior resulting from the physical processes of material separation and local fracture. For ductile materials, the relevant separation mechanism is micro-void nucleation, growth and coalescence, and the cohesive parameters can get a micromechanical interpretation [10]. The various functions for the cohesive law used in the literature [6] have in common, that they contain two characteristic parameters per crack opening mode, a cohesive strength, σ_{c}, and a critical separation, δ_{c}. In the present paper, only mode I fracture is considered and a rather versatile cohesive law, $\sigma_{\mathrm{n}}(\delta_{\mathrm{n}})$,

$$\sigma_{\mathrm{n}}(\delta_{\mathrm{n}}) = \sigma_{\mathrm{c}} \cdot \begin{cases} 2\left(\dfrac{\delta_{\mathrm{n}}}{\delta_1}\right) - \left(\dfrac{\delta_{\mathrm{n}}}{\delta_1}\right)^2 & \text{for } \delta_{\mathrm{n}} \le \delta_1 \\ 1 & \text{for } \delta_1 < \delta_{\mathrm{n}} \le \delta_2 \\ 2\left(\dfrac{\delta_{\mathrm{n}} - \delta_2}{\delta_{\mathrm{c}} - \delta_2}\right)^3 - 3\left(\dfrac{\delta_{\mathrm{n}} - \delta_2}{\delta_{\mathrm{c}} - \delta_2}\right)^2 + 1 & \text{for } \delta_2 \le \delta_{\mathrm{n}} \le \delta_{\mathrm{c}} \end{cases} \quad (1)$$

see Fig. 2a and [11], is applied, which contains two additional shape parameters, δ_1 and δ_2, The parameter δ_1 should be chosen as small as possible to obtain a high initial stiffness of the cohesive elements, as the deformation of the structure has to be dominated by the deformation of the solid elements only. The parameter δ_2 allows for a variation between deformation controlled, $\delta_2 \to \delta_1$, and an abrupt stress release, $\delta_2 \to \delta_{\mathrm{c}}$.

The interface elements are realised as user-defined elements, UEL, in the FE code ABAQUS for 2D and 3D applications, Fig. 2b, and they were particularly adapted to plane stress and shell structures by incorporating the change of element thickness [12, 13].

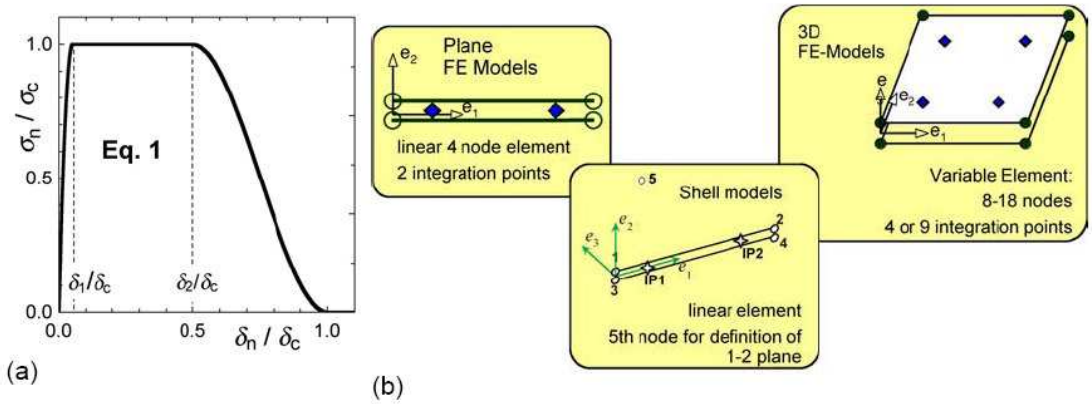

Fig. 2 – (a) Traction-separation law according to eq.(1) for δ_1 = 0.1 δ_c, δ_2 = 0.5 δ_c, (b) Interface elements in 2D and 3D structures

Alternatively to δ_c, the separation energy, Γ_c, which simply represents the area under the traction-separation curve,

$$\Gamma_c = \int_0^{\delta_c} \sigma_n(\delta_n)\, d\delta_n = \sigma_c \delta_c \left(\frac{1}{2} - \frac{1}{3}\frac{\delta_1}{\delta_c} + \frac{1}{2}\frac{\delta_2}{\delta_c} \right), \qquad (2)$$

can be introduced as a cohesive parameter. Estimates for the cohesive parameters in mode I fracture are the maximum true tensile stress at fracture of a notched tensile bar for the cohesive strength, σ_c, and the *J*-integral at crack initiation, J_i, for the separation energy, Γ_c, [6, 14]. A fine-tuning of the parameters by an FE simulation of a fracture mechanics test is recommended, however. Note, that the cohesive zone model is also applicable to the analysis of structures without cracks.
Beside mode I separation under remote tensile loading, the out-of-plane shear separation plays an important role in ductile fracture of thin panels. An extending crack commonly inclines to an angle of 45° to the remote loading direction, Fig. 3, thus inducing a local mode III field, a phenomenon known as "slant fracture" [15 - 17]. Within the methodology of plane-stress analyses of cracked panels by cohesive elements, slant fracture will be modelled as mode I separation with respectively modified "effective" cohesive parameters.

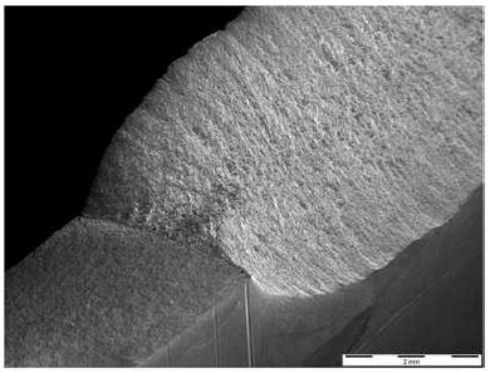

Fig. 3 - Slant fracture under remote mode I loading, material Al 5083.

2.2 Parameter Identification and Validation
The cohesive parameters are determined and validated for an aluminium alloy Al 5083 [18], which is used in shipbuilding and automotive industry. The thickness of the rolled panels is 3 mm. Various specimens have been manufactured from these panels, namely flat tensile specimens of 8 mm width for the determination of the stress-strain curve and fracture mechanics specimens of different sizes. The elastic properties are E = 70.3 GPa and ν = 0.33, and the proof stress is $R_{p0.2}$ = 242 MPa. Compact specimens, C(T), of widths W = 50 and 150 mm have been used to determine the cohesive parameters.

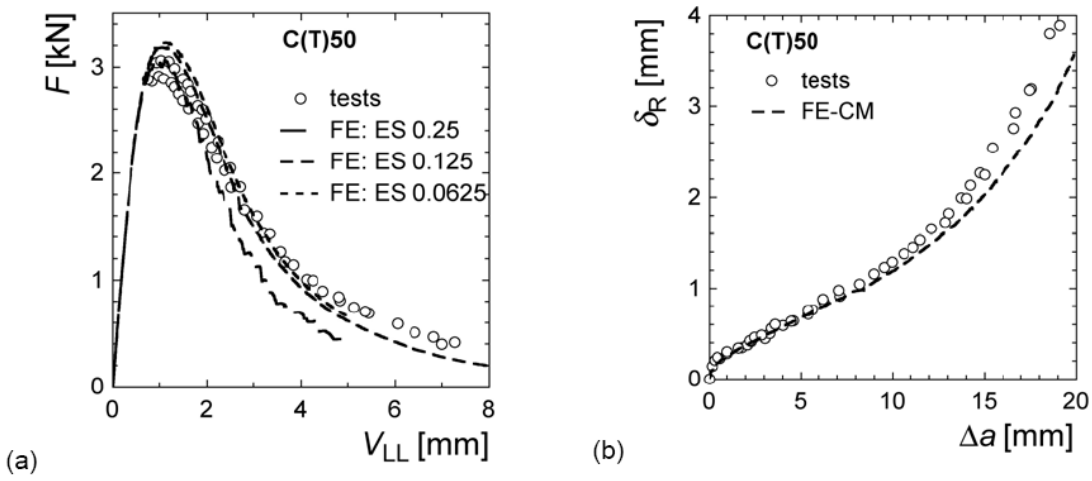

Fig. 4 - Parameter identification: test and simulation results of C(T) specimens, W = 50 mm, a_0/W = 0.5; (a) Load vs. load-line displacement curves, simulations in dependence on element size (0.25, 0.125, 0.0625 mm), (b) CTOD R-curve.

The shape parameters of the cohesive law were chosen as in Fig. 2a, resulting in $\Gamma_c = 0.75\sigma_c\delta_c$. An estimate of the cohesive strength, σ_c, was obtained from the normal stresses at fracture of flat tensile specimens, and the separation energy, Γ_c, was pre-estimated from the J-integral at beginning crack extension measured in the C(T) tests. Subsequent optimisation of the parameters by simulations of the load-displacement curve and the δ_R-curve of the C(T)50, see Fig. 4, yielded σ_c = 560 MPa and Γ_c = 10 kJ/m^2. The transferability of the model parameters to other specimen sizes and geometries like centre-cracked panels, M(T), has been verified in [18].
Mesh dependence of numerical results is a big issue in damage mechanics, when softening behaviour of materials is simulated. As the cohesive law is expressed in terms of stresses in dependence on the separation, see eq. (1), a length scale parameter is inherent to the model [10]. Thus, no pathological mesh dependence is expected, which could be verified by numerical simulations [19]. Fig 4a demonstrates the effect of the element size on the load-displacement curve of the C(T) specimen. A decreasing element length yields a convergent solution.

3. APPLICATION TO STRUCTURAL COMPONENTS

3.1 Stiffened Cylinder

Cylindrical shells with circumferential stiffeners under internal pressure may be regarded as simplified models of an aircraft fuselage. The following example, for which no experimental data is available, examine crack extension and residual strength of a shell containing a crack located between two stringers (one-bay crack), see Fig. 5. The FE model represents a 60° section of the total shell and accounts for symmetry.
The material is an aluminium alloy Al 6056 T78, which is considered as potential replacement of Al 2024, an alloy traditionally used for airplane fuselages. The material data and model parameters have been determined in a broad study of the strength and toughness properties of welded panels [20]. The shape parameters of the cohesive law were chosen as above.
The cohesive model offers some variability in the potential direction of crack extension, as cohesive elements may be placed along various paths. In the present example, the locations of cohesive elements allow for crack extension in three directions, along a surface line of the skin, through the stringer and in circumferential direction along the stringer, see Fig. 5a. The stringer thickness has been varied between t = 1.3 mm and 2.4 mm. The objective of this parameter study was to find out whether the crack continues extending in its original direction and thus ruptures the stringer or deviates and extends in circumferential direction along the stringer without penetrating it. Respective effects have been found on real structures.

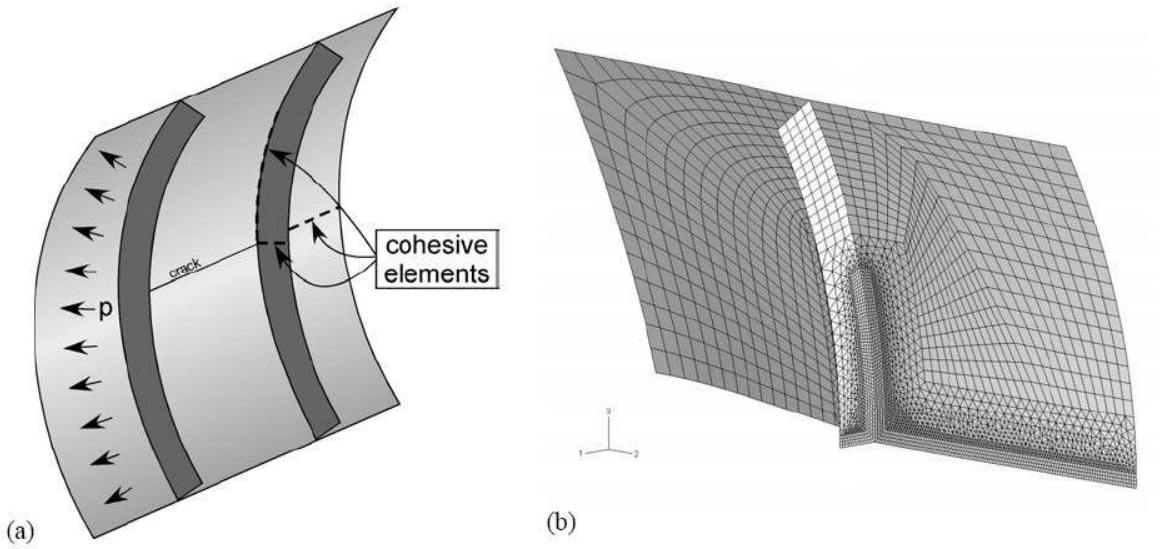

Fig. 5 - Stiffened cylinder with crack subject to internal pressure, diameter $2R$ = 100 mm, skin thickness t = 1 mm, distance of stringers $2W$ = 100 mm; (a) schematic of structure (b) FE model.

The pressure vs. CTOD curves for three values of stringer thickness, t, namely 1.3, 1.8 and 2.4 mm, are shown in Figure 6. The crack extension starts shortly before maximum load, i.e. below residual strength. The latter increases remarkably, when the stringer thickness changes from 1.3 mm to 1.8 mm. At the same time, the stability characteristic of the load-deformation behaviour alters. Whereas there is a smooth maximum for t = 1.3 mm, the load-displacement curve decreases steeply after its maximum for t = 1.8 mm, that means structural failure will occur abruptly. No significant further increase of maximum load is observed for t > 1.8 mm.

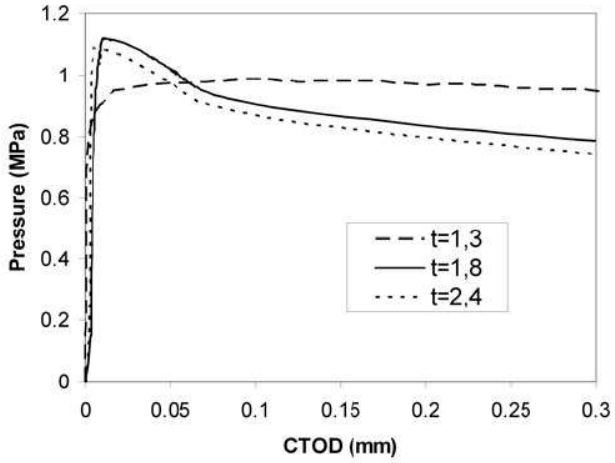

Fig. 5 - Stiffened cylinder with crack, pressure vs CTOD.

The increase of structural strength corresponds to a change of the crack path. For a stringer thickness of 1.3 mm the crack extends in its original direction in the shell structure and through the stringer, see Figure 6a. For stringer thicknesses of 1.8 mm and higher, the crack deviates at the stringer and extends circumferentially along the stringer without cutting it, see Figure 6b.
The studies of effects of the stringer stiffness may additionally be extended to effects of the bonding strength of the stringer to the skin. In this case, the stringer may also peel off as is observed in tests.

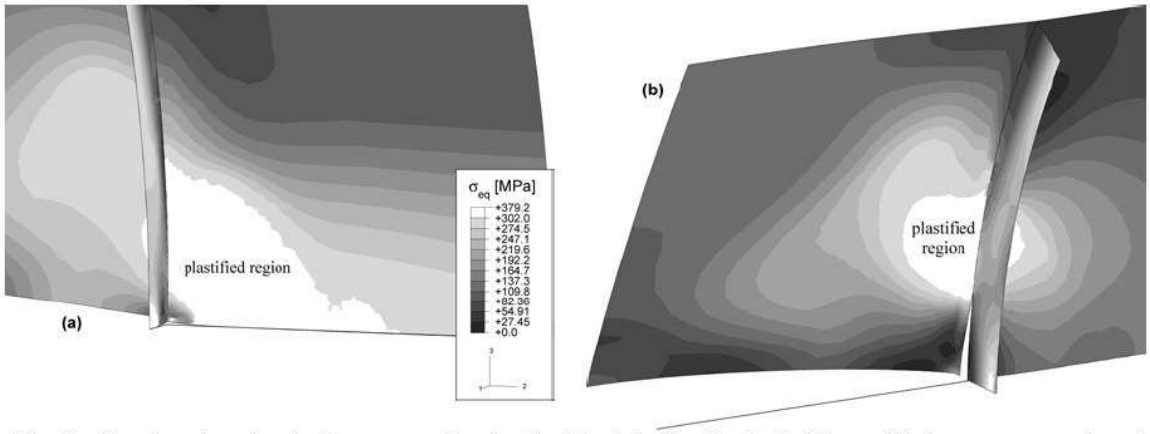

Fig. 6 - Crack extension in the pressurised cylindrical shell, effect of stringer thickness on crack path: (a) t = 1.3 mm, (b) t = 1.8 mm

3.2 IMA Fuselage Shell

The residual strength of airplane fuselages has to satisfy certification requirements. It has to be demonstrated that an as assumed crack will not be detrimental to the integrity under service conditions of internal cabin pressure. For this purpose, a longitudinal crack of twice the distance between two stiffeners (two-bay crack) is inserted into a barrel by fatigue loading. In the following static test under internal pressure, the cracked barrel has to endure at least 1.15 times the cabin pressure. Airbus Germany and IMA[1] have developed a respective test procedure. Instead of a complete barrel, only a shell section of 1/8th, i.e. 45°, is tested. The fuselage shell shown in Fig. 7a is part of a complete wide-body fuselage with an outer diameter of 5640 mm and 1.8 mm skin thickness. The shell is stiffened by 7 frames and 8 stringers. The boundary conditions applied to the shell section approximate the conditions in a complete barrel. The shell is subjected to internal pressure and biaxially loaded in circumferential and longitudinal directions. The applied edge forces represent the equilibrium situation in a closed stiffened cylinder.

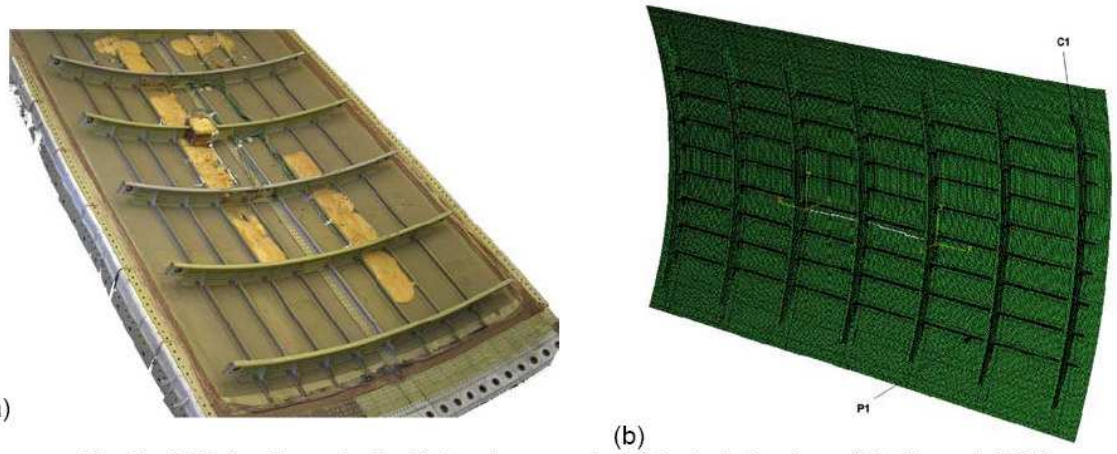

(a) (b)

Fig. 7 – IMA fuselage shell with two-bay crack: (a) tested structure, (b) FE model [21]

An FE model with 142500 “general purpose” shell elements and 972 cohesive elements was generated, Fig 7b. Internal pressure and boundary conditions were applied according to the situation in a pressurised closed cylinder, namely (i) axial forces acting as equilibrium forces to the pressure on the cylinder caps and (ii) only radial expansion of the circumferential edges being permitted. For details see [21, 22].

Fig. 8a shows the overall deformation of the shell magnified by a factor of 10, and Fig 8b the vicinity of the crack tip displaying the crack extension due to failed cohesive elements. No equilibrium has been found in the simulation at 95% of the experimentally measured failure pressure, though the global pressure vs CTOD curve did not exhibit a load maximum. As no respective deformation data of the

[1] IMA Materialforschung und Anwendungstechnik GmbH, Dresden

test is available, no comparison between experiment and simulation can be shown. The FE-analysis is hence only a feasibility study showing that the cohesive model can be applied to real large scale structures. The simulations [21, 22] also provided a detailed insight into the effects of the applied boundary conditions, which have to ensure that the tested fuselage section appropriately represents the situation of a complete, i.e. closed cylindrical fuselage.

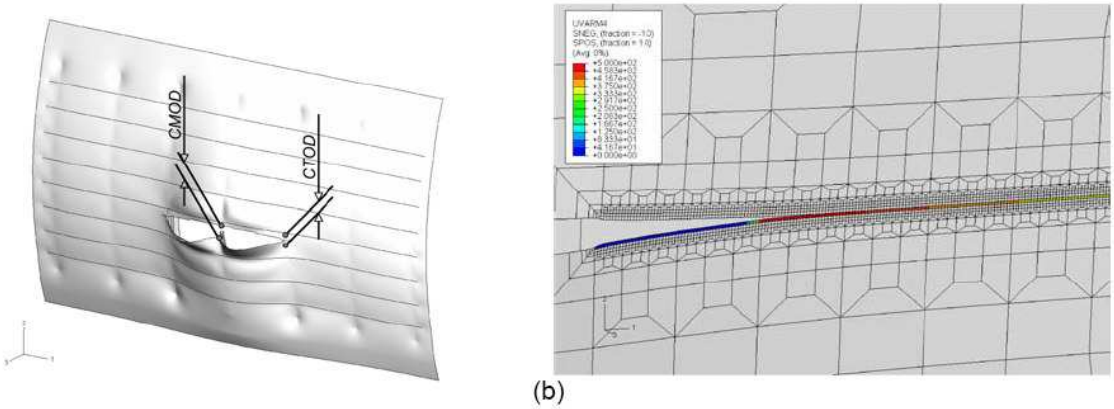

Fig. 8 – Deformed fuselage shell: (a) overall deformation (magnification factor 10), (b) vicinity of crack tip with failed cohesive elements.

3.3 ASTM Round Robin on Predicting Crack Growth in Integral Structures

The ASTM Task Group E08.04.05 organised a round robin aiming at the validation of analytical and numerical methods for predicting crack growth and residual strength in integral structures. For this purpose, a flat panel of thickness 7.6 mm with five stringers (Fig. 9) has been machined from a monolithic block of Al 2024-T351. It contains a fatigue crack that divides the central stringer. The tips of this initial crack are right ahead of the stringers #2 and #4, respectively. The panel is tested under quasi-static conditions. Crack branching along the skin and into the stringers occurs after initiation. Material properties, namely yield and ultimate strength, as well as a K_R-curve obtained from tests on M(T) specimens were provided. The results of the panel test have been handed out to the participants after they had submitted their predictions of the residual strength.

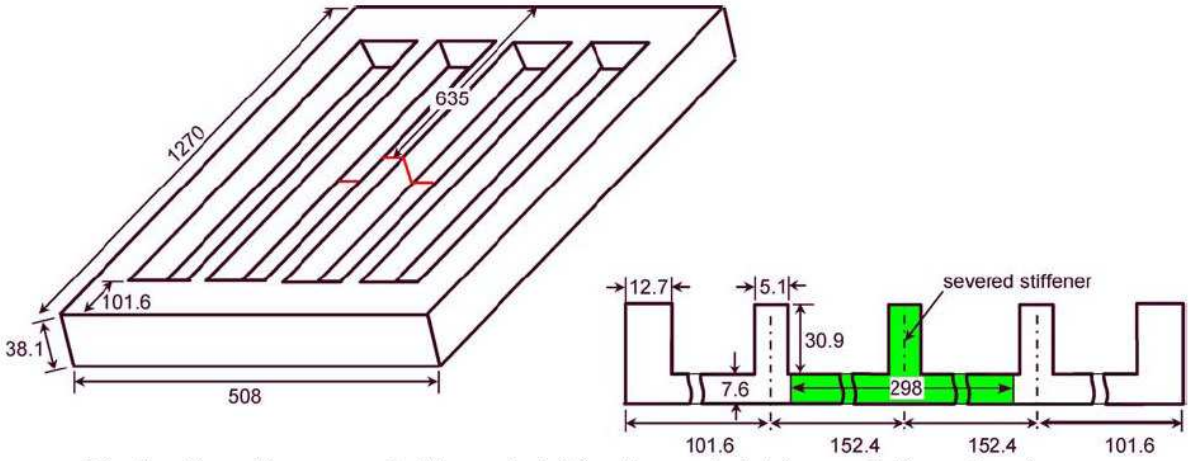

Fig. 9 – Five-stringer panel with crack dividing the central stringer; all dimensions in mm.

The present prediction has been achieved by finite element simulations with the cohesive model. First the cohesive parameters have been determined from a numerical simulation of the K_R-curve of the M(T) specimen as described in section 2.2. Then the five-stringer panel was modelled. It turned out that shell elements cannot reproduce the stress triaxiality at the junction between stiffener and skin correctly [23], which resulted in plastic collapse of the crack-tip shell elements rather than in crack extension, i.e. failure of the cohesive elements. Therefore 3D continuum elements had to be applied, though this means a vast increase of the model size and thus of computation time.
The model represents one quarter of the whole structure accounting for the symmetry conditions. Skin and stringer sections has been equipped with 2D cohesive elements, 15 over the stringer thickness and 24 over the skin thickness, yielding 4625 cohesive elements in total with a size of approximately

0.3×0.3 mm² each. The part of the ligament mesh arranged for crack extension is displayed in Fig. 10a. The whole structure contains 41294 continuum elements. As the panel model is 3D, the identification of the cohesive parameters required a 3D simulation of the M(T) specimen as well, resulting in Γ_c = 20 kJ/m^2 and σ_c = 970 MPa. Fig. 10b shows iso-contours of stress triaxiality, $h = \sigma_{hyd}/\sigma_{eff}$, for two stages of crack extension. Values of h > 1.5 are reached at the crack tip. The figure also displays the variation of local crack extension across the thickness, known as "tunnelling".

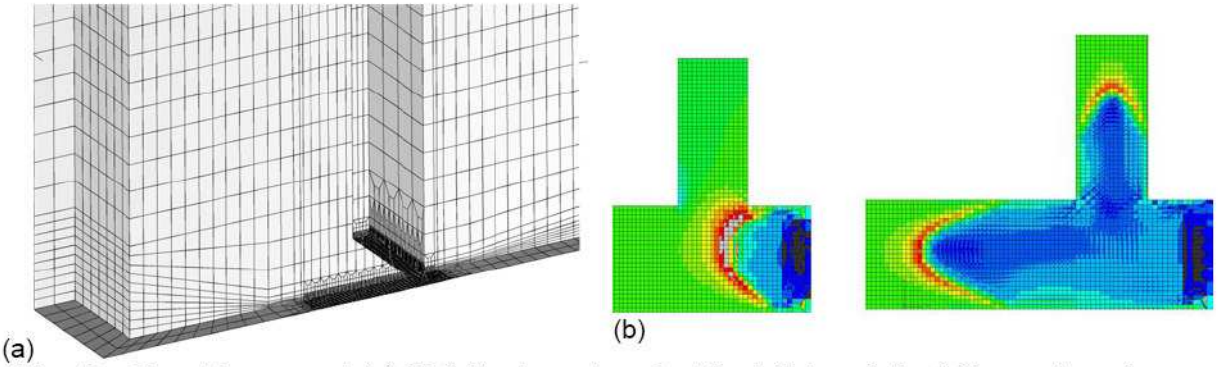

Fig. 10 – Five-stringer panel: (a) 3D finite element mesh at the initial crack tip, (b) iso-contours for extending crack.

The comparison of numerical and experimental load-displacement curves is shown in Fig. 11a. The residual strength obtained in the simulation is 135 MPa compared to 148 MPa in the test, which is a deviation of less than 9%. The prediction is conservative in the present case, which is a desirable attribute in structural assessment. It is not assured in general, however, that predictions will always be conservative.

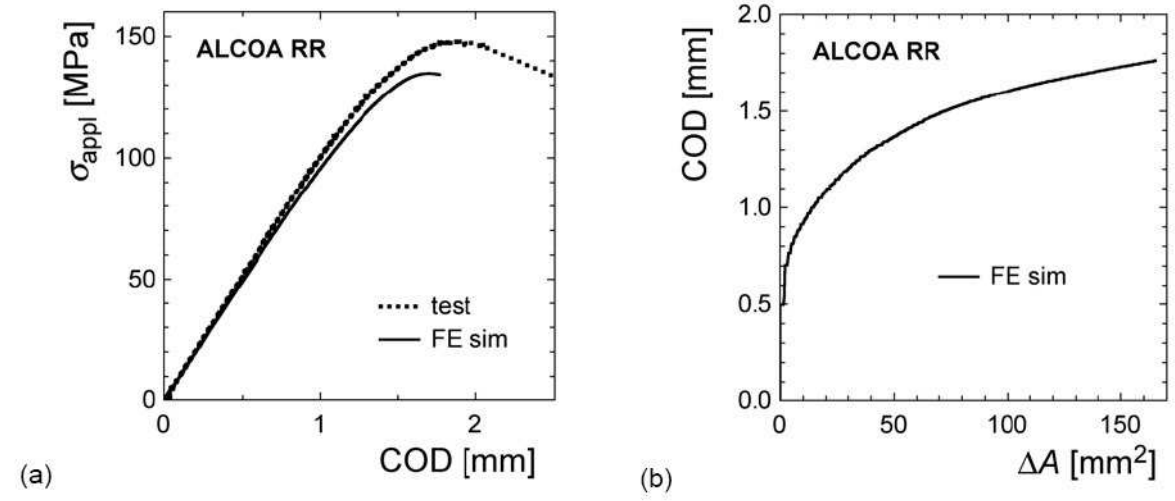

Fig. 11 – Five-stringer panel: (a) Applied stress vs COD, comparison between experimental and numerical results, (b) COD vs area of extending crack.

Some kind of (simulated) R-curve, namely COD in dependence of crack extension is displayed in Fig. 11b. As there are two crack fronts evolving at each side of the initial crack and as these crack fronts vary over the thickness, Fig. 10b, the total area of crack extension is plotted on the abscissa.

4 Summary and Conclusions

The cohesive model has proven its ability to predict crack extension and residual strength of components. Though only simulations of cracked structures have been presented here, cohesive models do not rely on the existence of an initial crack in general. This is an important advantage compared to fracture mechanics concepts.

Suitable meshing is crucial to realise the actual crack path. Cohesive interfaces are advantageous, when there is only a limited number of possibilities for the crack to grow. The model is numerically

stable for large crack extensions, it is not subject to any pathological mesh dependence like damage models and it provides physically meaningful parameters for characterizing strength and toughness of materials.

REFERENCES

[1] Newman JC, James MA, Zerbst U. A review of the CTOA/CTOD fracture criterion. Engng Fracture Mech 70, 2003; 371-85.
[2] Newman JC. Advances in fatigue and fracture mechanics analyses for aircraft structures. Proc. ICAF 2003; 3-42.
[3] Brocks W, Nègre P, Scheider I, Schödel M, Steglich D, Zerbst U. Structural integrity assessment by models of ductile crack extension in sheet metal. Steel Research 74, 2003; 504-513.
[4] Dugdale DS. Yielding of steel sheets containing slits. J Mech Phys Solids 8, 1960; 100-104.
[5] Barenblatt GI. The mathematical theory of equilibrium cracks in brittle fracture. Adv Appl Mech 7, 1962; 55-129.
[6] Brocks W, Cornec A, Scheider I. Computational aspects of nonlinear fracture mechanics. In: Milne, I, Ritchie, O, Karihaloo, B (eds.): Comprehensive structural integrity. Fracture of materials from nano to macro. Vol. 3, Oxford: Elsevier, 2003; 127-209.
[7] Chabanet O, Steglich D, Besson J, Heitmann V, Hellmann D, Brocks W.: Predicting crack growth resistance of aluminium sheets. Comp Mat Sci 26, 2003; 1-12.
[8] Roy YA, Dodds RH: Simulation of ductile crack growth in aluminium panels using 3-D surface cohesive elements. Int J Fract 110, 2001; 21-45.
[9] Siegmund T, Brocks W: Simulation of ductile crack growth in thin aluminum alloys. In: Halford GR, Gallagher JP (eds.): 31st Nat Symp Fatigue and Fracture Mechanics, Cleveland (OH, USA), ASTM STP 1389, 2000; 475 - 485.
[10] Brocks W. Cohesive strength and separation energy as characteristic parameters of fracture toughness and their relation to micromechanics. Structural Integrity and Durability 1, 2005; 233-244.
[11] Scheider I. Simulation of cup-cone fracture in round bars using the cohesive zone model. Proc. 1st MIT Conf. Computational Fluid and Solid Mechanics, Boston (MA, USA), 2000; 460-462.
[12] Brocks W, Scheider I: Cohesive elements for thin-walled structures. Comp Mat Sci 37, 2006; 101-109.
[13] Scheider I, Brocks W. Simulation of crack propagation and failure in shell structures using the cohesive model. In: Ramm, E, Wall, WA, Bletzinger, KU, Bischoff, M (eds.): Proc 5th Int. Conf. Computation of Shell and Spatial Structures. Salzburg (A), 2005.
[14] Cornec A, Scheider I, Schwalbe KH. On the practical application of the cohesive model. Engng Fracture Mech 70, 2003; 1963-87.
[15] Schroth JG, Hirth JP, Hoagland RG, Rosenfield AR. Combined Mode I-Mode III fracture of a high strength low-alloy steal. Metall Trans A 18A, 1987; 1061-1072
[16] Kamat SV, Hirth JP. A mixed mode I/III fracture toughness correlation. Scripta Metall Mater 30, 1994; 145-148.
[17] Mahgoub W, Deng X, Sutton MA. Three-dimensional stress and deformation fields around flat and slant cracks under remote Mode I loading conditions. Engng Fract Mech 70, 2003; 2527-2542.
[18] Scheider I, Schödel M, Brocks W, Schönfeld W. Crack propagation analyses with CTOA and cohesive model: Comparison and experimental validation, Engng Fracture Mech 73, 2006; 252-263.
[19] Brocks W, Scheider I, Schödel M. Simulation of crack extension in shell structures and prediction of residual strength. Arch Appl Mech 76, 2006; 655-665.
[20] Nègre P, Steglich D, Brocks W. Crack extension at an interface: prediction of fracture toughness and simulation of crack path deviation. Int J Fract 134, 2005; 209-229.
[21] Heartness S. Structural integrity analysis of an airplane fuselage section. Master Thesis, Report GKSS/WMS/05/07, GKSS Research Centre: 2005.
[22] Cornec A, Schönfeld W, Heartness S, Scheider I, Brocks W. Modellierung einer versteiften Flugzeugschale mit Zweifeldriss. Report GKSS/WMS/06/07, GKSS Research Centre: 2006.
[23] Scheider I, Brocks W. Residual strength prediction of a complex structure using crack extension analyses. Engng Fract Mech, submitted.